Journal of Alloys and Compounds 472 (2009) 59–64

Contents lists available at ScienceDirect

Journal of Alloys and Compounds

journal homepage: www.elsevier.com/locate/jallcom

Synthesis of In/InP core–shell nanospheres and their transformation into InP hollow nanospheres

Keyan Bao, Liang Shi, Shuzhen Liu, Shenglin Xiong, Xiaobo Hu, Yitai Qian*

Hefei National Laboratory for Physical Sciences at Microscale and Department of Chemistry, University of Science and Technology of China, Hefei, Anhui 230026, China

ARTICLE INFO

Article history:
Received 10 March 2008
Received in revised form 21 April 2008
Accepted 22 April 2008
Available online 3 June 2008

Keywords:
Nanostructures
Crystal growth
X-ray diffraction
Luminescence

ABSTRACT

Polycrystalline InP hollow nanospheres with an average size of 520 nm and shell thickness of about 110 nm were obtained by acid treatment of In/InP core–shell nanospheres which were solvothermally synthesized in ethanolamine–water binary solution at 180 °C. The sizes of InP hollow nanospheres increased with the increasing reactants quantities. Meanwhile the shell thicknesses of InP hollow nanospheres could be controlled by varying the quantity of yellow phosphorus. The process of In/InP core–shell nanospheres transforming into InP hollow nanospheres was also investigated. The InP products prepared in our experiments can emit blue light, which is different from previous reports and increases the potential application of InP nanomaterial.

1. Introduction

InP, an important III–V semiconductor with a direct band gap of 1.35 eV at room temperature, has a wide range of applications in electronic and optoelectronic devices such as high-speed logic circuits, millimetre-wave sources and amplifiers, and optical fibre communications [1–3]. Many reports showed that the shape, size and crystalline structure of semiconductors could greatly affect their physical and chemical properties [4,5]. Recently, hollow inorganic nanostructures have attracted considerable attention because of their promising applications, for example, nanoscale chemical reactors, efficient catalysts, and photonic building blocks [6,7].

A series of high temperature synthetic methods such as laser-assisted catalytic growth (LCG) [8–10], vapor–liquid–solid (VLS) [11] and thermal chemical process [12,13] were used to prepare InP nanostructures. And most of them are one-dimensional (1D) nanostructures. Meanwhile, InP nanostructures can also be synthesized in solution systems. For instance, InP nanocrystals were obtained under ultrasonic irradiation from the reaction of $InCl_3{\cdot}4H_2O$, yellow phosphorus and KBH_4 in a mixed solvents of ethanol and benzene [14], monodispersed InP quantum dots were synthesized via the reaction between In_2O_3 and yellow phosphorus in alkali aqueous [15], InP wires were prepared from the reaction of In_2O_3 and yellow phosphorus with CTAB as surfactant in aqueous solution [16], InP nanocrystals with rod-like morphologies were obtained using $InCl_3{\cdot}4H_2O$, yellow phosphorus and $NaBH_4$ as reactants and employing $C_{17}H_{35}CO_2K$ as surfactant in aqueous ammonia [17]. However, the synthesis of InP 3D nanostructures such as hollow nanospheres, and flowerlike architectures has rarely been reported.

Traditionally, the classic approaches for preparation of hollow spheres have focused on various sacrificial templates, including polystyrene spheres [18,19], silica spheres [20], resin spheres [21,22], vesicles [23] and liquid droplets [24,25]. Recently, some III–V semiconductors have also been prepared using the template method. For instance, Ga_2O_3 and GaN hollow spheres were obtained by using carbon spheres as templates [26]; InP honeycomb-like macroporous frameworks were fabricated from the reaction between $InCl_3{\cdot}4H_2O$ and yellow phosphorus employing Au as template in ethylenediamine solvent [27].

In this study, InP hollow nanospheres were obtained by acid treatment of In/InP core–shell nanospheres. The In/InP core–shell nanospheres were prepared in ethanolamine–water binary solution at 180 °C for 12 h. InP hollow nanospheres with different diameters and shell thicknesses could be prepared by varying the quantities of $InCl_3{\cdot}4H_2O$ and P_4. Furthermore, solid nanospheres and flowerlike architectures were also synthesized by controlling the reaction conditions.

2. Experimental

2.1. Synthesis of In/InP core–shell composite

In a typical synthesis, 2 mmol of $InCl_3{\cdot}4H_2O$ was dissolved in 5 mL of distilled water, and 40 mL of ethanolamine was added under stirring. Then 8 mmol of $NaBH_4$ and 10 mmol of yellow phosphorus (P_4) were added into the solution. The mix-

* Corresponding author. Tel.: +86 551 3601589; fax: +86 551 3607402.
E-mail address: bkeyan@mail.ustc.edu.cn (Y. Qian).

0925-8388/$ – see front matter © 2008 Elsevier B.V. All rights reserved.
doi:10.1016/j.jallcom.2008.04.076

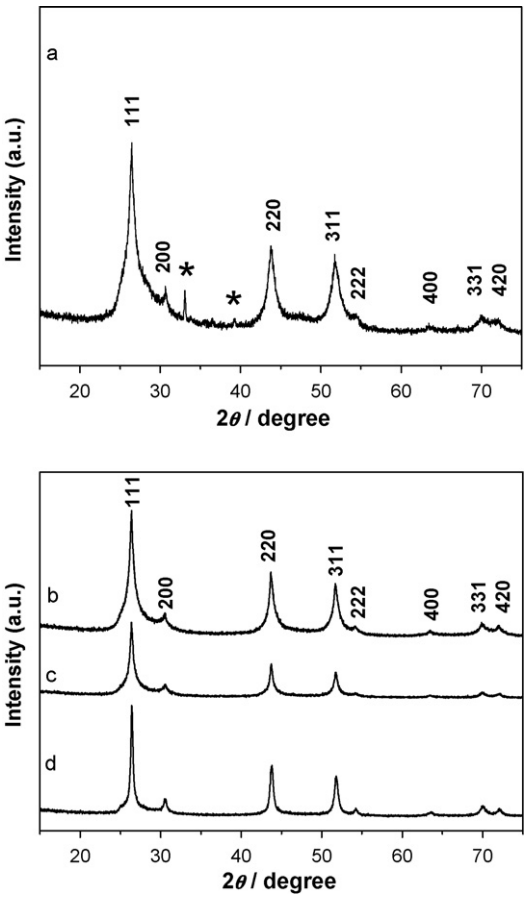

Fig. 1. XRD patterns of: (a) In/InP core–shell composite synthesized from the reaction between 2 mmol of $InCl_3{\cdot}4H_2O$ and 10 mmol of P_4 with $V_{EA} : V_{H_2O} = 8 : 1$. (*the excess metallic In). (b) InP hollow nanospheres obtained by acid treatment of In/InP core–shell composite at ambient temperature for 20 h. (c) InP solid nanospheres prepared by using 2 mmol of $InCl_3{\cdot}4H_2O$ and 25 mmol of P_4 as reaction materials with $V_{EA} : V_{H_2O} = 8 : 1$. (d) InP flowerlike architectures obtained via the reaction between 2 mmol of $InCl_3{\cdot}4H_2O$ and 25 mmol of P_4 with $V_{EA} : V_{H_2O} = 2 : 7$.

ture was transferred into a 50 ml Teflon-sealed autoclave and maintained at 180 °C for 12 h, and then cooled to room temperature naturally. The product was filtered and washed with distilled water and absolute alcohol several times, finally dried in vacuum at 60 °C for 2 h.

2.2. Synthesis of InP hollow nanospheres

InP hollow nanospheres were obtained by treating In/InP core–shell composite with dilute HCl (0.3 M) for 20 h at ambient temperature. The final product was washed with distilled water and absolute alcohol several times, and then dried in vacuum at 60 °C for 2 h.

2.3. Characterization

Powder X-ray diffraction (XRD) measurements were carried out with a Philips X'Pert diffractmeter (Cu Kα λ = 1.541874 Å; Nickel filter; 40 kV, 40 mA). FESEM images were taken on a JEOL JSM-6300F SEM. HRTEM images were performed on JEOL JEM-2010 microscope operating at 200 kV. PL measurements were taken at room temperature using a Fluorolog-3-TAU spectrofluorimeter (Jobin Yvon Company of France).

3. Results and discussion

Fig. 1a shows the X-ray diffraction (XRD) pattern of the as-prepared product synthesized from the reaction of 2 mmol of $InCl_3{\cdot}4H_2O$ and 10 mmol of P_4 with $V_{EA} : V_{H_2O} = 8 : 1$. The main reflection peaks can be indexed as zinc blende phase of InP with lattice constant $a = 5.873$ Å, which is in good agreement with the standard data (JCPDS PDF No. 32-0452, $a = 5.869$ Å). The two small diffraction peaks marked with stars at 32.9 and 39.4° can be indexed as (1 0 1) and (1 1 0) diffractions of metallic In (JCPDS PDF No. 05–0642, $a = 3.251$ Å). This indicates that the sample is a mixture of InP and metallic In. Fig. 1b is the XRD pattern of the above product treated by 0.3 M HCl for 20 h. It is obvious that after acid treatment only InP phase exists in the product. Fig. 1c and d shows the XRD patterns of InP solid nanospheres and InP flowerlike architectures. All the reflection peaks can be indexed as zinc blende phase of InP.

Fig. 2a shows the field-emission scanning electron microscopy (FESEM) image of the sample synthesized via the reaction between 2 mmol $InCl_3{\cdot}4H_2O$ of and 10 mmol of P_4 with $V_{EA} : V_{H_2O} = 8 : 1$. It is found that the sample is composed of nanospheres with sizes in the range of 500–550 nm and the surfaces of the nanospheres constructed out of small nanoparticles with an average size of 15 nm. Fig. 2b is the transmission electron microscopy (TEM) image of the sample, revealing that the sample consists of relatively uniform solid nanospheres. The corresponding selected-area electron diffraction (SAED) pattern (Fig. 2b, inset) indicates that the sample is polycrystalline and the diffraction rings from inside to outside can be indexed to (1 1 1), (2 2 0) and (3 1 1) diffractions of InP. However, the energy dispersive spectrometer (EDS) spectrum (Fig. 2c) reveals the presence of excess In in the nanospheres (In/P atomic ratio of 1.68:1; the signals of Cu, C and Cr come from the copper grid used for the HRTEM observation). And the XRD pattern (Fig. 1a) also suggests that the product consists of InP and metallic In. Namely, the product is In/InP composite.

Fig. 2d shows the FESEM image of the product obtained from acid treatment of In/InP composite for 20 h. From Fig. 2d many nanospheres and their inner cavities can be observed clearly, confirming the hollow structure of the as-obtained product. The TEM image (Fig. 2e) also reveals that the as-obtained product is hollow nanospheres with sizes in the range of 500–600 nm and shell thickness of about 100 nm. The corresponding SAED pattern (Fig. 2e, inset) indicates that the sample is polycrystalline and the diffraction rings from inside to outside can be indexed as (1 1 1), (2 2 0) and (3 1 1) diffractions of InP. The EDS spectrum (Fig. 2f) reveals the presence of In and P elements at an In/P atomic ratio of 1.03:1 (the signals of Cu, C and Cr come from the copper grid used for the HRTEM observation). The XRD pattern also confirms that only InP phase exists in the product (Fig. 1b). That is to say, the product is InP hollow nanospheres. Now, it is clear that the product was In/InP core–shell nanospheres and InP hollow nanospheres could be obtained by acid treatment of In/InP core–shell nanospheres.

In addition, InP hollow nanospheres prepared under different reaction conditions were also studied. It was found that the reactant quantities had a dramatic effect on the diameters and shell thicknesses of InP hollow nanospheres. For example, when the quantities of $InCl_3{\cdot}4H_2O$ and P_4 were increased to 4 mmol and 16 mmol, respectively, InP hollow nanospheres with diameters in the range of 700–900 nm and shell thickness of about 90 nm were prepared (Fig. 3a). As shown in Fig. 3b, when the quantities of $InCl_3{\cdot}4H_2O$ and P_4 were decreased to 1 mmol and 7 mmol respectively, small InP hollow nanospheres with an average size of 430 nm and wall thicknesses of 80–90 nm were obtained. Meanwhile, the shell thicknesses of InP hollow nanospheres could be controlled by varying the quantity of yellow phosphorus when the quantity of $InCl_3{\cdot}4H_2O$ was fixed at 2 mmol. For instance, InP hollow nanospheres with diameters in the range of 500–600 nm and shell thickness of about 70 nm (Fig. 3c) were synthesized with a low quantity of yellow phosphorus (8 mmol P_4). When the quantity of yellow phosphorus was increased to 13 mmol, InP hollow nanospheres with an average size of 560 nm and wall thickness of about 150 nm were prepared (Fig. 3d).

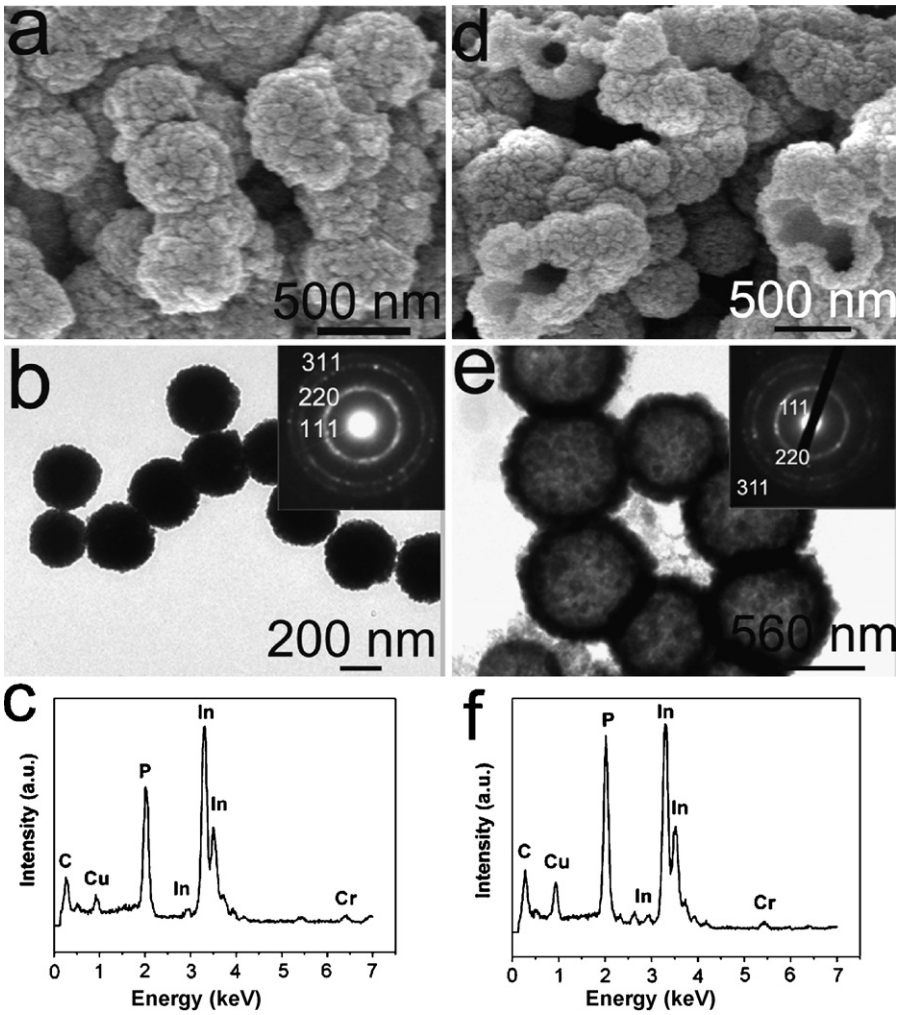

Fig. 2. (a) FESEM image; (b) TEM image and corresponding SAED pattern; (c) EDS spectrum (In:P = 1.68:1) of In/InP core–shell nanospheres. (d) FESEM image; (e) TEM image and corresponding SAED pattern; (f) EDS spectrum (In:P = 1.03:1) of InP hollow nanospheres prepared by treatment of In/InP core–shell composite with dilute HCl at ambient temperature for 20 h.

Interestingly, InP solid spheres were obtained without acid treatment when the quantity of yellow phosphorus was increased to 25 mmol ($InCl_3{\cdot}4H_2O$: 2 mmol). The corresponding XRD patterns (Fig. 1c and d) confirm that the products are pure InP. Two kinds of morphologies of InP were obtained by controlling the volume ratio of EA/H_2O. Fig. 4a and b shows the FESEM and TEM images of the sample synthesized via the reaction between 2 mmol of $InCl_3{\cdot}4H_2O$ and 25 mmol of P_4 with $V_{EA} : V_{H_2O} = 8 : 1$. It is found that the sample consists of solid nanospheres with sizes in the range of 500–600 nm and the surfaces of the solid nanospheres constructed out of small nanoparticles about 12 nm. InP flowerlike architectures were synthesized when the ratio of EA/H_2O was decreased to 7:2. As shown in Fig. 4c, the sample is composed of a large quantity of flowerlike patterns with an average size of about 1 mm and the flowers are composed of nanodollops with an average size of 160 nm. The flowerlike structure of the product was further investigated by SAED and HRTEM. Fig. 4d exhibits the TEM image of a single nanodollop about 150 nm in size. The inset of Fig. 4e shows the SAED pattern of the nanodollop, which indicates that the nanodollop is single crystal. The high-resolution transmission electron microscopy (HRTEM) image in Fig. 4f also indicates the good crystallinity of the nanodollop. The crystal planes have lattice spacing of about 2.06 Å corresponding to (2 2 0) plane of the InP crystal.

The process of In/InP core–shell nanospheres transformation into InP hollow nanospheres was also investigated. Fig. 5a–c shows the TEM images of the products which were obtained via acid treatment of In/InP core–shell nanospheres for 2, 10 and 20 h. Fig. 5a reveals that dilute HCl has slightly corroded the product. As shown in Fig. 5b, more and more metallic In was dissolved and some interstitial spaces appeared when the acid treatment time was prolonged to 10 h. But there was still some metallic In remaining in the centres of the nanospheres. When the treatment time was increased to 20 h, the obvious contrast between the dark edges and the relatively bright centres verified their hollow structures (Fig. 5c).

Based on the above investigations, the formation process of InP hollow nanospheres can be proposed as follows. At the first step, In^{3+} was reduced to metallic In by $NaBH_4$. The reaction temperature (180 °C) was higher than the melting points of In and P_4 (157 °C and 44.1 °C, respectively), but lower than their boiling points (2080 °C and 280 °C, respectively). A little amount of InP was formed via the reaction of the reduced liquid metallic In and liquid P_4. The newly formed InP coated on the outer surfaces of aggregated metallic In particles. When P_4 was exhausted, In/InP core–shell structure was formed. The reaction can be suggests as follows:

$$2InCl_3 + 6NaBH_4 \rightarrow 2In + 6NaCl + 6BH_3 + 3H_2$$

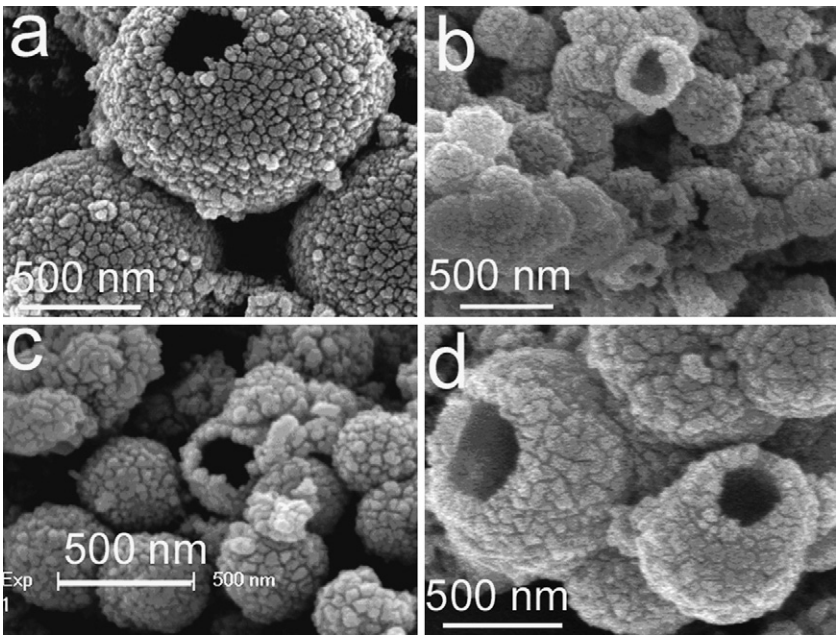

Fig. 3. (a–d) SEM images of InP hollow nanospheres prepared with $V_{EA} : V_{H_2O} = 8 : 1$ and different quantities of $InCl_3 \cdot 4H_2O$ and P_4 (mmol): (a) 4 and 16; (b) 1 and 6; (c) 2 and 8; (d) 2 and 13.

$$4In + P_4 \rightarrow 4InP$$

When removing the unreacted In by treatment with dilute HCl, the inner In disappeared and InP hollow nanospheres were formed. The growth process of InP hollow nanospheres is simply described in Scheme 1.

4. Optical property

The room-temperature photoluminescence (PL) spectra of the as-synthesized InP hollow nanospheres, solid nanospheres and flowerlike architectures were measured. InP hollow nanospheres show an emission band at 433 nm (Fig. 6a). InP solid nanospheres exhibit an emission peak near 432 nm and flowerlike architectures reveal an emission peak at 412 nm, as shown in Fig. 6b and c, respectively. These peaks indicate that the samples have pronounced blueshift in contrast to the bulk InP (direct band gap 918 nm, 1.35 eV, 300 K) [28]. One possible cause for this blueshift is the compressive stress that results from lattice distortion of these ethanolamine-capping nanoparticles. The exact mechanism of luminescence is not clear at present and further study is under way. Previous reports had shown that InP nanostructures usually emitted red light [13,16,29,30]. However, the InP products prepared

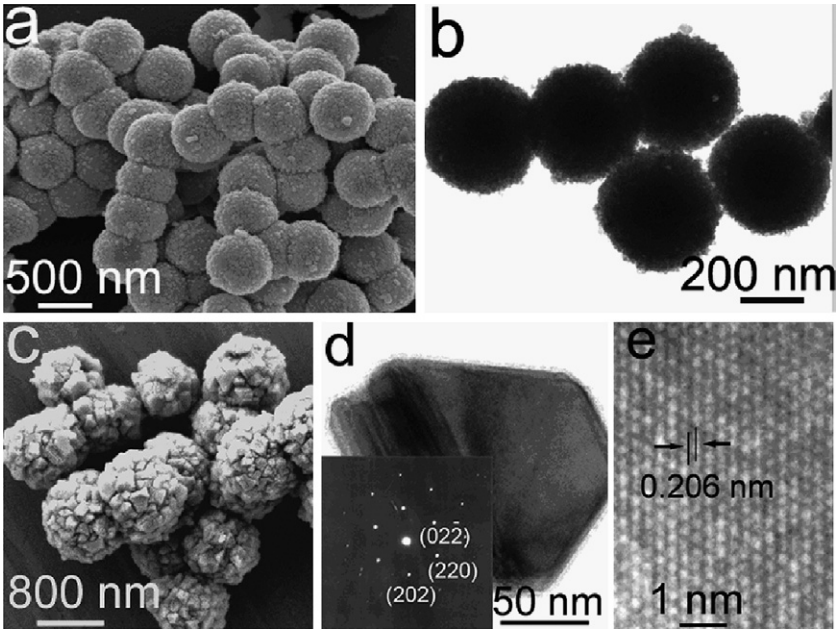

Fig. 4. (a) SEM and (b) TEM images of InP solid nanospheres prepared with $V_{EA} : V_{H_2O} = 8 : 1$. (c) SEM; (d) TEM and (e) HRTEM images of InP flowerlike architectures synthesized with $V_{EA} : V_{H_2O} = 7 : 2$.

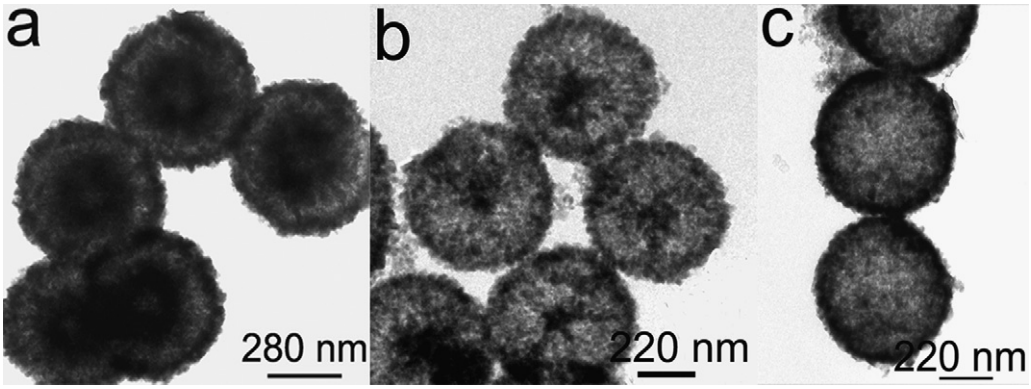

Fig. 5. TEM images of the product in the formation of InP hollow nanospheres by treatment of In/InP core–shell composite with dilute HCl under different reaction time (h): (a) 2; (b) 10; (c) 20.

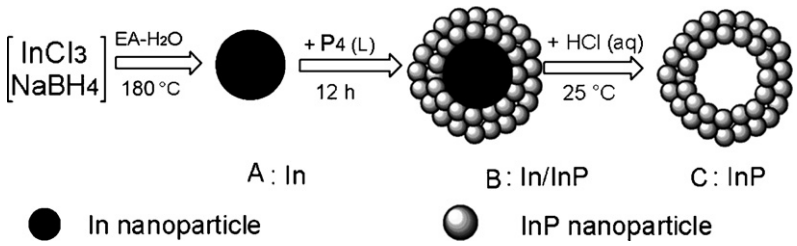

Scheme 1. Schematic illustration of the formation process of InP hollow nanosphere. (A) A In nanoparticle was formed in the initial solvothermal process. (B) The metallic In reacted with P_4 and formed In/InP core–shell structure. (C) A final InP hollow nanosphere was obtained by treatment In/InP core–shell composite with 0.3 M HCl.

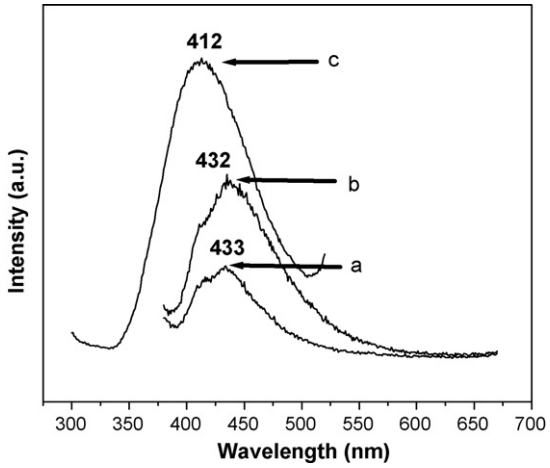

Fig. 6. Room-temperature photoluminescence (pL) spectra of: (a) InP hollow nanospheres (excitation at 275 nm); (b) InP solid nanospheres (excitation at 275 nm); (c) InP flowerlike architectures (excitation at 336 nm).

in our experiments can emit blue light, which is different from the previous reports and increases the potential applications of InP nanomaterial.

5. Conclusions

In summary, by controlling the reaction conditions such as the volume ratio of EA/H_2O and the reactants quantities, InP hollow nanospheres, solid nanospheres and flowerlike architectures were synthesized via the reactions between $InCl_3{\cdot}4H_2O$ and P_4 in ethanolamine–water binary solution at 180 °C for 12 h. In detail, when yellow phosphorus was insufficiency, In/InP core–shell nanospheres were synthesized and after acid treatment InP hollow nanospheres were obtained. The sizes and shell thicknesses of InP hollow nanospheres could be controlled by varying the quantities of $InCl_3{\cdot}4H_2O$ and P_4. When yellow phosphorus was abundant, InP solid spheres were prepared without acid treatment. InP solid nanospheres and flowerlike architectures could be obtained by changing the volume ratio of EA/H_2O. The optical properties of InP hollow nanospheres, solid nanospheres and flowerlike architectures were also investigated by the photoluminescence spectra.

Acknowledgements

The financial support of this work, by National Natural Science Foundation of China (No. 20431020), the 973 Project of China (No. 2005CB623601) and the China Postdoctoral Science Foundation (No. 20070420124), is gratefully acknowledged.

References

[1] T. Kawakami, M. Okamura, Electron. Lett. 15 (1979) 502–504.
[2] K. Kamimura, T. Suzuki, A. Kumioka, Appl. Phys. Lett. 38 (1981) 259–261.
[3] H. Carrere, X. Marie, T. Amand, Appl. Phys. Lett. 89 (2006) 181115.
[4] C.M. Lieber, Solid State Commun. 107 (1998) 607–616.
[5] A.P. Alivisatos, Science 271 (1996) 933–937.
[6] Q. Peng, Y.J. Dong, Y.D. Li, Angew. Chem. Int. Ed. 42 (2003) 3027–3030.
[7] Y.G. Sun, B. Mayers, Y.N. Xia, Adv. Mater. 15 (2003) 641–646.
[8] X.F. Duan, Y. Huang, Y. Cui, J.F. Wang, C.M. Lieber, Nature 409 (2001) 66–69.
[9] J.F. Wang, M.S. Gudiksen, X.F. Duan, Y. Cui, C.M. Lieber, Science 293 (2001) 1455–1457.
[10] X.F. Duan, C.M. Lieber, Adv. Mater. 12 (2000) 298–302.
[11] E.P.A.M. Bakkers, M.A. Verheijen, J. Am. Chem. Soc. 125 (2003) 3440–3441.
[12] G.Z. Shen, Y. Bando, C.Y. Zhi, X.L. Yuan, T. Sekiguchi, D. Golberg, Appl. Phys. Lett. 88 (2006) 243106.
[13] G.Z. Shen, Y. Bando, B.D. Liu, C.C. Tang, D. Golberg, J. Phys. Chem. B 110 (2006) 20129–20132.
[14] B. Li, Y. Xie, J.X. Huang, Y. Liu, Y.T. Qian, Ultrason. Sonochem. 8 (2001) 331–334.
[15] S.M. Gao, J. Lun, Y. Xie, Chem. Commun. 24 (2002) 3064–3065.
[16] Y.J. Xiong, Y. Xie, Z.Q. Li, X.X. Li, S.M. Gao, Chem. Eur. J. 10 (2004) 654–660.
[17] S. Wei, J. Lu, Y.T. Qian, J. Appl. Phys. 95 (2004) 3683–3688.
[18] F. Caruso, R.A. Caruso, H.M. Khwald, Science 282 (1998) 1111–1114.
[19] Z.Z. Yang, Z.W. Niu, Y.F. Lu, Z.B. Hu, C.C. Han, Angew. Chem. 42 (2003) 1943–1945.

[20] S.W. Kim, M. Kim, W.Y. Lee, T. Hyeon, J. Am. Chem. Soc. 124 (2002) 7642–7643.
[21] A. Bourlinos, N. Boukos, D. Petridis, Adv. Mater. 14 (2002) 21–24.
[22] A.B. Bourlinos, M.A. Karakassides, D. Petridis, Chem. Commun. 16 (2001) 1518–1519.
[23] H.T. Schmidt, A.E. Ostafin, Adv. Mater. 14 (2002) 532.
[24] T. Nakashima, N. Kimizuka, J. Am. Chem. Soc. 125 (2003) 6386–6387.
[25] X.Y. Gao, J.S. Zhang, L. Zhang, Adv. Mater. 14 (2002) 290.
[26] X.M. Sun, Y.D. Li, Angew. Chem. 43 (2004) 3827–3831.
[27] X.W. Zheng, C.Z. Liu, Y. Xie, Eur. J. Inorg. Chem. 12 (2006) 2364–2369.
[28] R. Newman, Phys. Rev. 111 (1958) 1518.
[29] S. Kan, T. Mokari, E. Rothenberg, U. Banin, Nat. Mater. 2 (2003) 155–158.
[30] D. Battaglia, X.G. Peng, NanoLett. 2 (2002) 1027–1030.